2011

A Few Transient Effects in AT-Cut Quartz Thickness-Shear Resonators

Runyu Zhang
University of Nebraska-Lincoln

Hongping Hu
Huazhong University of Science and Technology, hphu@yahoo.cn

Correspondence

A Few Transient Effects in AT-Cut Quartz Thickness-Shear Resonators

Runyu Zhang and Hongping Hu

***Abstract*—We study a few transient effects of AT-cut quartz thickness-shear resonators, including resonator turning on and turning off as well as voltage amplitude and frequency fluctuations. Mindlin's two-dimensional plate equations are used and solved analytically. Both a sudden change and a gradual change of the driving voltage are studied. It is found that for a resonator with a frequency of 1.649430868 MHz and material quality factor of $Q = 10^5$, the characteristic time scale of the transient effects is of the order of 0.1 s.**

I. Introduction

Piezoelectric crystals are widely used to make resonators for time-keeping, frequency generation and operation, telecommunication, and sensing. Quartz is the most widely used crystal for resonator applications. A large portion of quartz resonators operate with the so-called thickness-shear (TSh) vibration modes of a plate [1], [2]. The frequencies of these modes are mainly determined by the plate thickness, in contrast to the usual extensional or flexural modes of plates used in structural engineering whose frequencies are strongly dependent on the plate length and width. Because the plate thickness is much smaller than the length or width, the TSh modes used in crystal plate resonators have much higher frequencies and are therefore called high-frequency modes. These modes can be conveniently excited by an electric field in the plate thickness direction produced by a voltage across a pair of electrodes at the plate top and bottom. Quartz TSh resonators have been the subject of sustained study. TSh vibrations of quartz plates, elastic or piezoelectric, were analyzed in some early papers [1]–[4]. The effects of electrodes separated from the plate surfaces and the related air gaps between the electrodes and the plate were studied in [5]. When a thin layer of a different material is deposited on a crystal plate resonator, the TSh frequencies are lowered because of the inertia of the additional mass layer. This effect has broad applications in mass sensors, quartz crystal microbalances [6]–[9], and the design of the electrodes on quartz resonators [10]–[13]. TSh-mode quartz resonators have also received wide attention as fluid sensors for viscosity/density measurement [14]–[18]. Recently, the effects of microparticles on TSh quartz resonators were investigated in [19] for particle characterization.

In all of the analyses in [1]–[19], only time-harmonic TSh motions of a quartz plate resonator were considered. Although a time-harmonic analysis can provide the most basic frequency behaviors of a quartz resonator, including resonant frequencies and mode shapes, there are transient effects important in resonator operations that cannot be described by time-harmonic solutions. For example, resonator turning on or turning off are avoidable transient processes. When a resonator is in harmonic operation, fluctuations of the driving voltage also induce transient effects. The accurate prediction and control of these transient effects are of fundamental importance for better resonator performance.

In this paper, we analyze theoretically a few basic transient effects in TSh quartz plate resonators. Because of material anisotropy and electromechanical coupling, theoretical analysis of quartz resonators is usually very complicated mathematically. We use the two-dimensional equations for thin piezoelectric plates developed by Mindlin [20] which have proven to be very effective in theoretical analyses of quartz TSh resonators.

II. Governing Equation

Consider a thin piezoelectric plate of rotated Y-cut quartz with thickness $2b$ and density ρ as shown in Fig. 1. Rotated Y-cuts include the most widely used AT-cut as a special case. The length $2a$ and width $2c$ of the plate are much larger than the thickness. The plate normal is along the x_2 axis. The x_1 and x_3 axes are in the middle plane of the plate. We neglect edge effects and consider pure thickness modes, independent of x_1 and x_3. The plate is effectively unbounded in the x_1–x_3 plane. It is electroded at $x_2 = \pm b$, with a driving voltage $V(t)$ applied across the electrodes. The electrode thickness and density are neglected. TSh modes can exist in an infinite quartz plate of rotated Y-cut quartz alone without couplings to other modes. We consider the fundamental TSh mode and employ the first-order theory by Mindlin [20]. In this theory, the displacement field of the fundamental TSh mode is approximated by [20]

$$u_1 \cong u_1(x_2, t) \cong x_2 u_1^{(1)}(t), \quad u_2 \cong 0, \quad u_3 \cong 0. \qquad (1)$$

From [20, Eq. (30)], for pure TSh modes in an unbounded plate, setting all derivatives with respect to x_1 and x_3 to zero, we obtain the following ordinary differential equation governing $u_1^{(1)}(t)$:

Manuscript received July 16, 2011; accepted October 3, 2011. This work was supported by the National Science Foundation of China (Nos. 10872074 and 10932004) and the Major State Basic Research Development Program of China (973 Program) (Grant No. 2009CB724205).

R. Zhang is with the Department of Mechanical and Materials Engineering, University of Nebraska, Lincoln, NE.

H. Hu is with the Department of Mechanics, Huazhong University of Science and Technology, Wuhan, China (e-mail: hphu@yahoo.cn).

Digital Object Identifier 10.1109/TUFFC.2011.2140

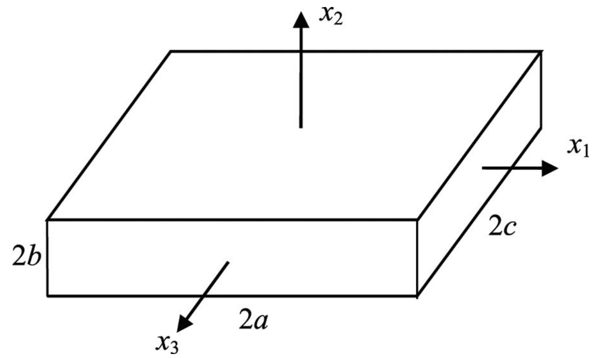

Fig. 1. A rotated Y-cut quartz plate and coordinate system.

$$-3b^{-2}(\kappa_1^2 c_{66} u_1^{(1)} + \kappa_1 e_{26} \phi^{(1)}) = \rho \ddot{u}_1^{(1)}, \tag{2}$$

where c_{66} and e_{26} are the relevant elastic and piezoelectric constants. For an electroded plate, the shear correction factor κ_1 in (2) is given by [20]

$$\kappa_1^2 = \frac{\pi^2}{12}\left(1 - \frac{8}{\pi^2} k_{26}^2\right), \quad k_{26}^2 = \frac{e_{26}^2}{\varepsilon_{22}\hat{c}_{66}}, \quad \hat{c}_{66} = c_{66} + \frac{e_{26}^2}{\varepsilon_{22}}, \tag{3}$$

where ε_{22} is the relevant dielectric constant. In (2), the first-order plate electric potential $\phi^{(1)}(t)$ is related to the driving voltage $V(t)$ through [20]

$$\phi^{(1)} = \frac{1}{2b} V(t). \tag{4}$$

Substitution of (4) into (2) yields

$$\ddot{u}_1^{(1)} + \omega_0^2 u_1^{(1)} + c\dot{u}_1^{(1)} = \alpha V(t), \tag{5}$$

where we have denoted

$$\omega_0^2 = 3b^{-2}\kappa_1^2 c_{66}/\rho, \quad \alpha = -3\kappa_1 e_{26}/(2\rho b^3). \tag{6}$$

ω_0 is the resonant frequency of the fundamental TSh mode. In (5), we have introduced a damping term, $c\dot{u}_1^{(1)}$, in the manner of [21] with the damping coefficient

$$c = 2\omega_0\zeta = \omega_0/Q, \tag{7}$$

where ζ is the relative damping coefficient and Q is the material quality factor.

III. Sudden Changes of Driving Voltage

Consider the sudden application of a time-harmonic driving voltage on a resonator at rest when $t = t_0$. The initial-value problem consists of (5) with the applied voltage

$$V(t) = \begin{cases} 0, & t < t_0, \\ \bar{V}\exp(i\omega t), & t \geq t_0, \end{cases} \tag{8}$$

and initial data

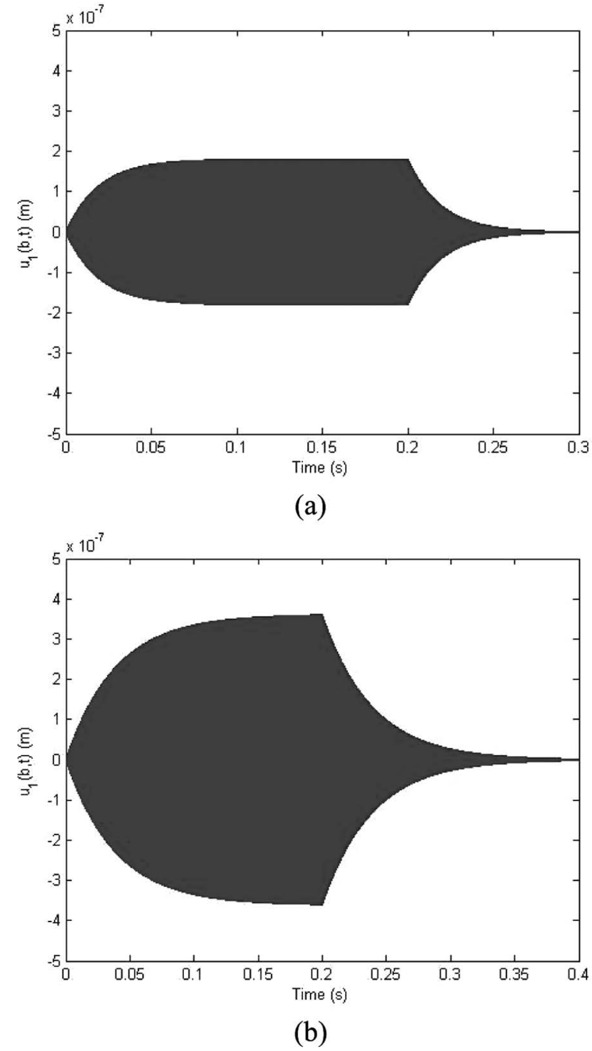

Fig. 2. Effects of damping on resonator turning on and off: (a) $Q = 10^5$, (b) $Q = 2 \times 10^5$.

$$u_1^{(1)}(t_0) = u_0, \quad \dot{u}_1^{(1)}(t_0) = v_0, \tag{9}$$

where $\bar{V}$ is a constant. The solution to the initial-value problem can be obtained in a straightforward manner. The result can be written as

$$u_1^{(1)}(t) = C_1\exp(\lambda_1 t) + C_2\exp(\lambda_2 t) + C_3\exp(i\omega t), \tag{10}$$

where

$$\lambda_{1,2} = \frac{-c \pm i\sqrt{4\omega_0^2 - c^2}}{2}. \tag{11}$$

The C_1 and C_2 terms are the transient part and the C_3 term is the steady-state part of the solution. They depend on the initial data and the driving term, respectively, in addition to ω_0 and c.

For numerical results, we consider a quartz plate with a thickness of $2b = 1$ mm. The material constants of AT-cut quartz can be found in [22]. For quartz, Q is of the order of 10^5. We use $Q = 10^5$ except in Fig. 2(b). The amplitude of the driving voltage $\bar{V} = 1$ V except in Fig. 4. In this case, the fundamental thickness-shear frequency $\omega_0 = 1.649430868$ MHz. The corresponding period is 6.0627×10^{-7} s. We examine the displacement of the plate top surface (where the displacement is large) versus time, i.e., $u_1(b, t)$.

Fig. 2 shows the result when the resonator is turned on at $t = 0$ s with $u_0 = 0$ and $v_0 = 0$, and then turned off at $t = 0.2$ s for two different values of Q. The driving frequency $\omega = \omega_0 = 1.649430868$ MHz. During the time interval shown, the resonator goes through many cycles. The curve of $u_1(b, t)$ makes many turns and effectively fills an area whose boundary is the envelope of the $u_1(b, t)$ curve. In Fig. 2(a), the amplitude of the surface displacement starts from zero, increases monotonically, and then reaches steady-state vibration in about 0.1 s. During 0.1 s, the resonator goes through 1.6494×10^5 cycles. We note the difference in the convexity of the envelope of the turning on and turning off processes. In Fig. 2(b), because the damping is about half of that in Fig. 2(a), the amplitude is larger. For smaller damping, it takes longer for the resonator to reach steady-state or come to rest as expected because the effect of initial data dies out more slowly.

Fig. 3 shows the turning on and off of resonators with different resonant frequencies. For Fig. 3(a), $b = 1$ mm and $\omega = \omega_0 = 0.82472$ MHz. For Fig. 3(b), $b = 1.5$ mm and $\omega = \omega_0 = 0.54981$ MHz. Clearly, a thicker resonator with a lower frequency has a longer transition time.

In Fig. 4, we show the effect of a sudden and temporary rise of the amplitude of the driving voltage. The driving frequency is still $\omega = \omega_0 = 1.649430868$ MHz. At $t = 0.2$ s, $\bar{V}$ is increased from 1 to 1.5 V, and then at $t = 0.3$ s, $\bar{V}$ is decreased back to 1 V. The amplitude of the voltage fluctuation is exaggerated so that it can be seen clearly in the figure. The behavior is similar to that in Fig. 2, except that the displacement begins with and goes back to a steady-state amplitude instead of zero.

Fig. 5 shows the effect of a sudden increase of the driving frequency by 10 Hz between $t = 0.2$ s and $t = 0.35$ s for a resonator which is already in steady-state motion. This 10 Hz of deviation from the resonant frequency is a realistic number because typical frequency shifts in resonators are of the order of ppm (parts per million). The time scale of the transient processes of the amplitude drop and rise is about 0.1 s. When the driving frequency is off by 10 Hz, the displacement amplitude decreases significantly, almost by one half. We also note that in this case, the convexity of the amplitude drop and rise are the same.

IV. Gradual Changes of Driving Voltage

The sudden change of the driving voltage analyzed in the previous section is an idealization of a real voltage change, which always takes a small amount of time to occur. In this section, we analyze the more realistic situation in which the voltage change has a characteristic time τ. The case of a sudden voltage change can be viewed as a

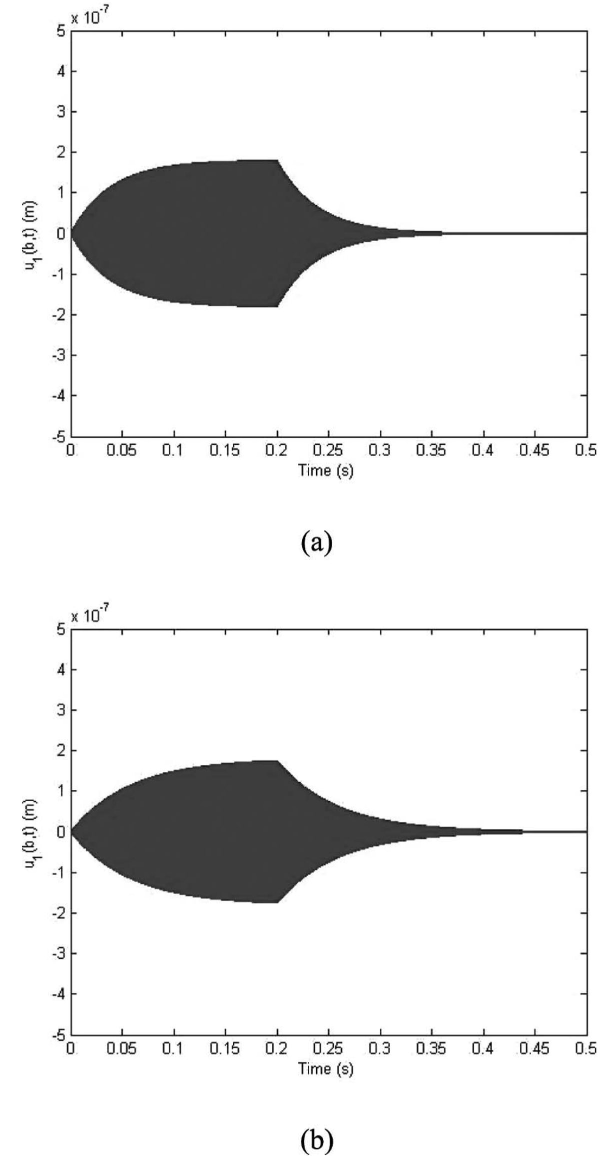

Fig. 3. Effects of resonant frequency on resonator turning on and off: (a) $\omega_0 = 0.82472$ MHz, (b) $\omega_0 = 0.54981$ MHz.

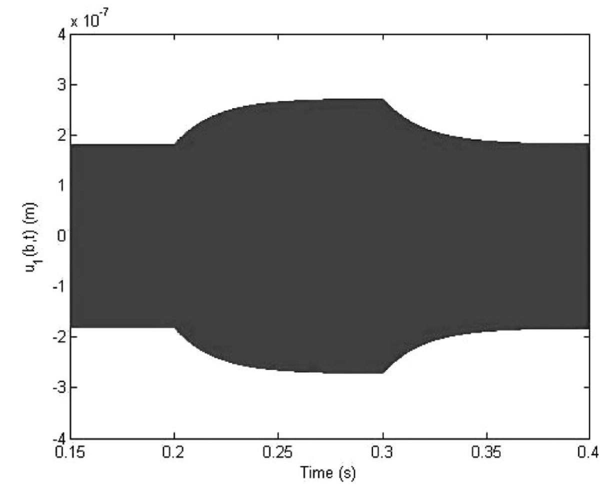

Fig. 4. Effects of driving voltage amplitude fluctuation.

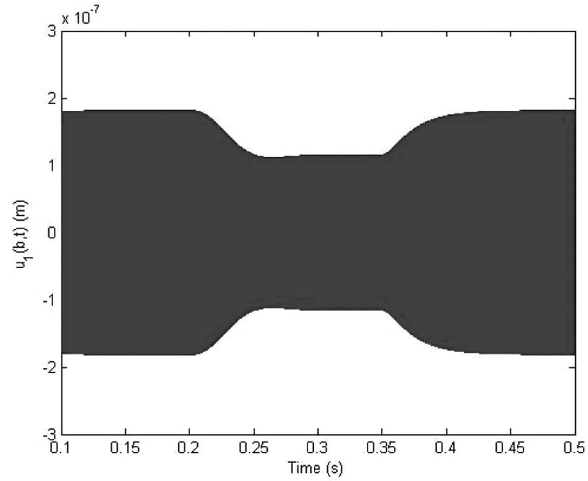

Fig. 5. Effects of driving voltage frequency fluctuation.

special case with $\tau = 0$. Specifically, consider the resonator turning-on process with the following applied voltage and initial data:

$$V(t) = \begin{cases} 0, & t < 0, \\ (1 - e^{-t/\tau})\bar{V}\exp(i\omega t), & t \geq 0, \end{cases} \tag{12}$$

$$u_1^{(1)}(0) = 0, \quad \dot{u}_1^{(1)}(0) = 0. \tag{13}$$

The solution of (5) under the conditions of (12) and (13) can be found as

$$u_1^{(1)}(t) = C_1\exp(\lambda_1 t) + C_2\exp(\lambda_2 t) + C_3\exp(i\omega t) + C_4\exp\left[\left(i\omega - \frac{1}{\tau}\right)t\right], \tag{14}$$

where C_1 through C_4 are constants depending on the parameters in (5), (12), and (13). We plot (14) for three different values of $\tau = 0$ s, 10^{-4} s, and 2×10^{-4} s in Figs. 6(a), 6(b), and 6(c), respectively. When $\tau = 0$ s, the resonator begins to vibrate noticeably immediately after the driving voltage is applied, as seen in Fig. 6(a). In Figs. 6(b) and 6(c), the resonator is slower to start, and the displacement amplitude grows more slowly.

V. Conclusion

Simple analytical solutions are obtained from Mindlin's first-order plate equations for transient vibrations of an AT-cut quartz TSh resonator. The solution shows that the typical response time for the resonator to adjust to a sudden change of the driving voltage amplitude or frequency is of the order of 0.1 s when the frequency is 1.649430868 MHz and the material Q is 10^5. For higher Q or lower resonant frequency, the response time becomes longer. When the driving frequency is off resonance by 10 Hz, the vibration amplitude is decreased by about one half.

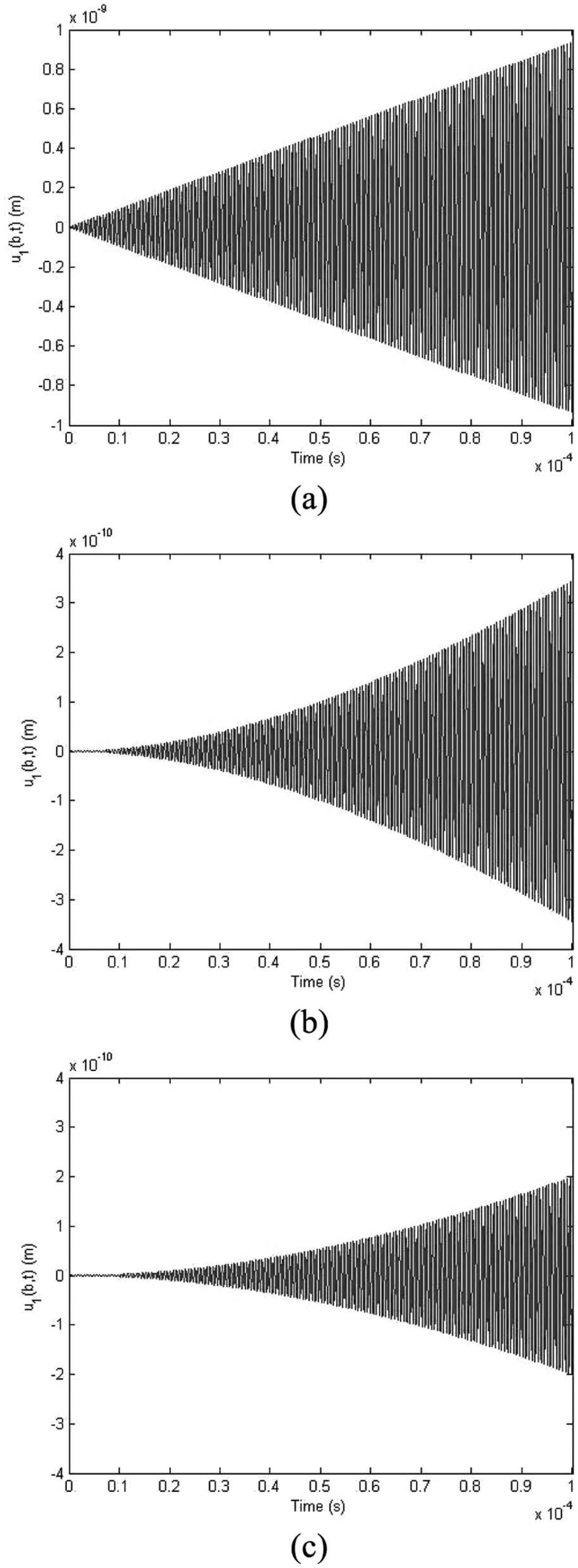

Fig. 6. Effects of gradually changing driving voltage: (a) $\tau = 0$ s, (b) $\tau = 10^{-4}$ s, (c) $\tau = 2 \times 10^{-4}$ s.

Acknowledgment

The authors thank Professor J. Yang of the University of Nebraska–Lincoln for suggesting this study.

References

[1] I. Koga, "Thickness vibrations of piezoelectric oscillating crystals," *Physics*, vol. 3, no. 2, pp. 70–80, 1932.

[2] H. F. Tiersten, "Thickness vibrations of piezoelectric plates," *J. Acoust. Soc. Am.*, vol. 35, no. 1, pp. 53–58, 1963.

[3] J. L. Bleustein and H. F. Tiersten, "Forced thickness-shear vibrations of discontinuously plated piezoelectric plates," *J. Acoust. Soc. Am.*, vol. 43, no. 6, pp. 1311–1318, 1968.

[4] H. F. Tiersten, "A corrected modal representation of thickness vibrations in quartz plates and its influence on the transversely varying case," *IEEE Trans. Ultrason. Ferroelectr. Freq. Control*, vol. 50, no. 11, pp. 1436–1443, 2003.

[5] Z. T. Yang, S. H. Guo, Y. T. Hu, and J. S. Yang, "Thickness-shear vibration of rotated y-cut quartz plates with unattached electrodes and asymmetric air gaps," *Philos. Mag. Lett.*, vol. 89, no. 5, pp. 313–321, 2009.

[6] V. G. Sauerbrey, "Verwendung von schwingquarzen zur wägung dünner schichten und zur mikrowägung," *Z. Phys.*, vol. 155, no. 2, pp. 206–222, 1959.

[7] R. D. Mindlin, "High frequency vibrations of plated, crystal plates," in *Progress in Applied Mechanics* (the Prager anniversary volume), New York: Macmillan, 1963, pp. 73–84.

[8] J. G. Miller and D. J. Bolef, "Acoustic wave analysis of the operation of quartz-crystal film-thickness monitors," *J. Appl. Phys.*, vol. 39, no. 12, pp. 5815–5816, 1968.

[9] F. Boersma and E. C. van Ballegooyen, "Rotated Y-cut quartz crystal with two different electrodes treated as a one-dimensional acoustic composite resonator," *J. Acoust. Soc. Am.*, vol. 62, no. 2, pp. 335–340, 1977.

[10] J. A. Kosinski, "Thickness vibration of flat piezoelectric plates with massy electrodes of unequal thickness," in *Proc. IEEE Ultrasonics Symp.*, 2003, pp. 70–73.

[11] J. Wang and L. J. Shen, "Exact thickness-shear resonance frequency of electroded piezoelectric crystal plates," *J. Zhejiang Univ. Sci.*, vol. 6, no. 9, pp. 980–985, 2005.

[12] J. S. Yang, H. G. Zhou, and W. P. Zhang, "Thickness-shear vibration of rotated Y-cut quartz plates with relatively thick electrodes of unequal thickness," *IEEE Trans. Ultrason. Ferroelectr. Freq. Control*, vol. 52, no. 5, pp. 918–922, 2005.

[13] J. S. Yang, Y. T. Hu, Y. Zeng, and H. Fan, "Thickness-shear vibration of rotated Y-cut quartz plates with imperfectly bounded surface mass layers," *IEEE Trans. Ultrason. Ferroelectr. Freq. Control*, vol. 53, no. 1, pp. 241–245, 2006.

[14] K. K. Kanazawa and J. G. Gordon II, "The oscillation frequency of a quartz resonator in contact with a fluid," *Anal. Chim. Acta*, vol. 175, no. 1, pp. 99–105, 1985.

[15] C. E. Reed, K. K. Kanazawa, and J. H. Kaufman, "Physical description of a viscoelastically loaded AT-cut quartz resonator," *J. Acoust. Soc. Am.*, vol. 68, no. 5, pp. 1993–2001, 1990.

[16] S. J. Martin, V. E. Granstaff, and G. C. Frye, "Characterization of a quartz crystal microbalance with simultaneous mass and liquid loading," *Anal. Chem.*, vol. 63, no. 20, pp. 2272–2281, 1991.

[17] Y. Jing, J. Chen, X. Chen, and X. Gong, "Frequency shift of thickness-shear vibrations of AT-cut quartz resonators due to a liquid layer with the electrode stiffness considered," *IEEE Trans. Ultrason. Ferroelectr. Freq. Control*, vol. 54, no. 7, pp. 1290–1292, 2007.

[18] B. Liu, Q. Jiang, and J. S. Yang, "Fluid-induced frequency shift in a piezoelectric plate driven by lateral electric fields," *Int. J. Appl. Electromagn. Mech.*, vol. 34, no. 3, pp. 171–180, 2010.

[19] C. L. Zhang, N. Liu, J. S. Yang, and W. Q. Chen, "Thickness-shear vibration of AT-cut quartz plates carrying finite-size particles with rotational degree of freedom and rotatory inertia," *IEEE Trans. Ultrason. Ferroelectr. Freq. Control*, vol. 58, no. 3, pp. 666–670, 2011.

[20] R. D. Mindlin, "High frequency vibrations of piezoelectric crystal plates," *Int. J. Solids Struct.*, vol. 8, no. 7, pp. 895–906, 1972.

[21] J. S. Yang, X. M. Yang, J. A. Turner, J. A. Kosinski, and R. A. Pastore Jr., "Two-dimensional equations for electroelastic plates with relatively large shear deformations," *IEEE Trans. Ultrason. Ferroelectr. Freq. Control*, vol. 50, no. 7, pp. 765–772, 2003.

[22] H. F. Tiersten, "Analysis of intermodulation in thickness-shear and trapped energy resonators," *J. Acoust. Soc. Am.*, vol. 57, no. 3, pp. 667–681, 1975.